Revision of Model Parameters for κ-Type Charge Transfer Salts: An *Ab Initio* Study

Hem C. Kandpal, Ingo Opahle, Yu-Zhong Zhang, Harald O. Jeschke,* and Roser Valentí

Institut für Theoretische Physik, Goethe-Universität Frankfurt, Max-von-Laue-Straße 1, 60438 Frankfurt am Main, Germany

(Received 5 April 2009; published 4 August 2009)

Intense experimental and theoretical studies have demonstrated that the anisotropic triangular lattice as realized in the κ-(BEDT-TTF)$_2X$ family of organic charge transfer salts yields a complex phase diagram with magnetic, superconducting, Mott insulating, and even spin liquid phases. With extensive density functional theory calculations we refresh the link between many body theory and experiment by determining hopping parameters of the underlying Hubbard model. This leads us to revise the widely used semiempirical parameters in the direction of less frustrated, more anisotropic triangular lattices. The implications of these results on the systems' description are discussed.

DOI: 10.1103/PhysRevLett.103.067004 PACS numbers: 74.70.Kn, 71.10.Fd, 71.15.Mb, 71.20.Rv

A strong research trend of the new millennium has been the desire to understand complex many body phenomena like superconductivity and magnetism by realistic modeling, i.e., to employ precise first principles calculations to feed the intricate details of real materials into the parameter sets of model Hamiltonians that are then solved with increasingly powerful many body techniques. The κ-(BEDT-TTF)$_2X$ [1] organic charge transfer salts are a perfect example for a class of materials with such fascinating properties that they drive progress in experimental and many body methods alike. Experimentally, the phase diagram shows Mott insulating, superconducting, magnetic, and spin liquid phases [2–5]. Theoretically, the underlying anisotropic triangular lattice is a great challenge due to effects of frustration and the intense efforts to get a grip on the problem include studies with path integral renormalization group (PIRG) [6], exact diagonalization [7], variational Monte Carlo calculations [8], cluster dynamical mean field theory [9,10], and dual fermions [11] to cite a few. In this rapidly expanding field of research, electronic structure calculations play the decisive role of mediating between the complex underlying structure and phenomenology of organic charge transfer salts and the models used for understanding the physics [12], and in this Letter, we will provide the perspective of precise, state of the art electronic structure calculations.

Previously, κ-type charge transfer (CT) salts have been investigated by semiempiricial and first principles electronic structure calculations. The most commonly used t, t', U parameter sets derive from extended Hückel molecular orbitals calculations [13,14] performed on different constellations of BEDT-TTF dimers.

The main result reported here is that our first principles study shows all four considered κ-type CT salts to be *less* frustrated than previously assumed based on semiempirical theory. Most importantly, the often cited value of $t'/t = 1.06$ [13] for the spin liquid material κ-(ET)$_2$Cu$_2$(CN)$_3$ should be replaced by the significantly smaller value $t'/t = 0.83 \pm 0.08$. This has fundamental implications on the systems' model description as we shall see below.

In this Letter, we employ the Car-Parrinello [15] projector-augmented wave [16] molecular dynamics (CPMD) method for relaxing the only partially known structures and perform structure optimizations at constant pressure [17] in order to prepare high pressure structures. We calculated the electronic structure using two full-potential all-electron codes, the linearized augmented plane wave (LAPW) method implemented in WIEN2K [18], and the full-potential local-orbital (FPLO) method [19].

We base our study on the following structures: For κ-(BEDT-TTF)$_2$Cu$_2$(CN)$_3$, the crystal structure [20] was published without hydrogen atom positions; we add them and perform a CPMD relaxation within the generalized gradient approximation (GGA) in which we keep lattice parameters and heavy atom (S, Cu) positions fixed [21]. With this procedure we make sure that the important atomic positions in the crystal structure remain as given by the diffraction measurements. We remove the inversion center in the middle of a cyano group by lowering the symmetry from $P2_1/c$ to Pc. No high pressure structures of κ-(BEDT-TTF)$_2$Cu$_2$(CN)$_3$ are published, and we therefore perform a full relaxation of the structure and lattice parameters at a pressure $P = 0.75$ GPa [22]; we recover the Pc symmetry by further optimizing the high pressure structure with symmetry constraints. For κ-(BEDT-TTF)$_2$Cu(SCN)$_2$, structures at ambient pressure and at $P = 0.75$ GPa are known [23]. Ambient pressure structures are available for κ-(BEDT-TTF)$_2$Cu[N(CN)$_2$]Br [24,25] and κ-(BEDT-TTF)$_2$Cu[N(CN)$_2$]Cl [26]. We will refer to the four materials as κ-CN, κ-SCN, κ-Br and κ-Cl for brevity. At ambient pressure and low temperatures κ-SCN and κ-Br superconduct while κ-Cl orders antiferromagnetically.

As an example for the structure of all κ-type CT salts considered here, we show in Fig. 1 the structure of κ-CN. The strongly anisotropic nature of the materials is apparent from the alternation of charge donating ET layers and acceptor anion layers [Fig. 1(a)], Cu$_2$(CN)$_3$ in this case. Experimental observations [13] as well as our calculations

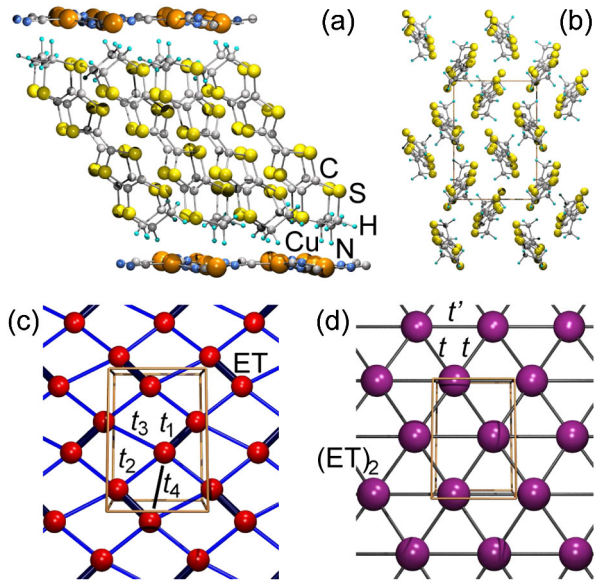

FIG. 1 (color online). Structure of κ-(BEDT-TTF)$_2$Cu$_2$(CN)$_3$ as typical example of the κ-type CT salts. (a) Side view with ET layers separated by insulating Cu$_2$(CN)$_3$ anion layers. (b) ET lattice, viewed in the bc plane. The unit cell containing four ET molecules is shown. (c) ET lattice shown in the same projection as (b) where the ET molecules have been replaced by single spheres. ET dimers are emphasized by heavier bonds. (d) Lattice of ET dimers, replaced by single spheres.

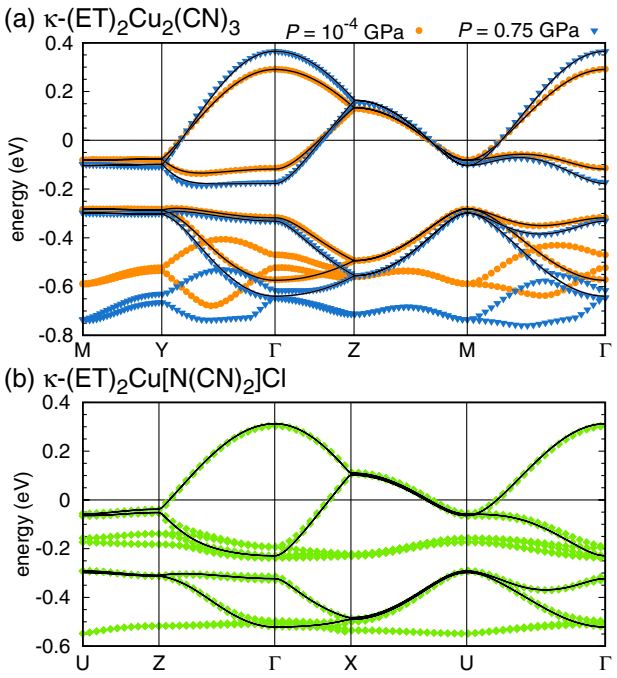

FIG. 2 (color online). DFT band structures of (a) κ-(BEDT-TTF)$_2$Cu$_2$(CN)$_3$ at ambient pressure and at $P =$ 0.75 GPa, and of (b) κ-(BEDT-TTF)$_2$Cu[N(CN)$_2$]Cl shown with symbols. Lines represent the tight-binding fits to the bands close to E_F deriving from ET molecules.

show that Cu occurs in Cu^{+1} oxidation state here and has a filled 3d shell, making the anion layers insulating. The κ-type arrangement of ET molecules [Fig. 1(b)] exhibits a strong dimerization of the molecules, four of which are contained in a unit cell. They form the lattice shown in simplified form in [Fig. 1(c)]. In the charge transfer process, each molecule donates a charge of $-0.5e$ and is left with half a hole. Considering pairs of dimers as the fundamental unit leads to the triangular lattice of Fig. 1(d) with one hole per dimer.

In Fig. 2 we show three examples of low energy band structures for κ-CN at ambient and elevated pressure [Fig. 2(a)] and for κ-Cl [Fig. 2(b)]. The overall features of the band structures are very similar to the known semiempirical band structures, with two antibonding bands of the ET molecules crossing the Fermi level, and the corresponding bonding bands nearly mirror symmetric below. Because of the double number of eight ET molecules per unit cell in the case of κ-Cl, Fig. 2(b) actually has four bands crossing the Fermi level, which are pairwise degenerate due to the high symmetry ($Pnma$) of the crystal structure. In contrast to previous calculations, there are four bands with mainly Cu 3d character close to the ET bands: slightly below the bonding ET bands in the case of κ-CN and slightly below the antibonding ET bands in the case of κ-Cl. The band structures of Fig. 2(a) were performed with LAPW using the GGA functional [27]. We checked the reliability and reproducibility of these results by repeating the calculation with FPLO [29], and we found that the band structures and all derived quantities match very well. As κ-Cl has roughly twice as many atoms in the unit cell compared to κ-CN, we used the faster FPLO method, within GGA, for Fig. 2(b). The low energy bands show almost no dispersion in the direction perpendicular to the anion layers which is the a direction (M-Y in the Brillouin zone) for κ-CN and the b direction (U-Z in the Brillouin zone) for κ-Cl, confirming the quasi-two-dimensional character of the κ-type CT salts.

We corroborated that the calculated band structures agree with experimental evidence by calculating the Fermi surface (FS) for κ-CN at ambient pressure and at $P = 0.75$ GPa. The FS consists of two different sheets arising from the two bands crossing the Fermi energy, a corrugated cylinder around Z and a quasi-one-dimensional sheet parallel to M-Y. Both sheets touch along the line M-Z and give rise to a combined elliptical orbit (Fig. 3) which encloses 99%–100% of the area of the first Brillouin zone. This is in good agreement with previous calculations [13] and with angle-dependent magnetoresistance oscillations (AMRO) measurements [30]. Our calculated FS shows the same behavior with pressure as observed in experiment. The area enclosed by the combined elliptical orbit increases by 6% from 37.4 nm^{-2} at ambient pressure to 39.7 nm^{-2} at $P = 7.5$ kbar (see Fig. 3), which is consistent with the increase of 6% between 2.1 and 7 kbar obtained from AMRO measurements in Ref. [30].

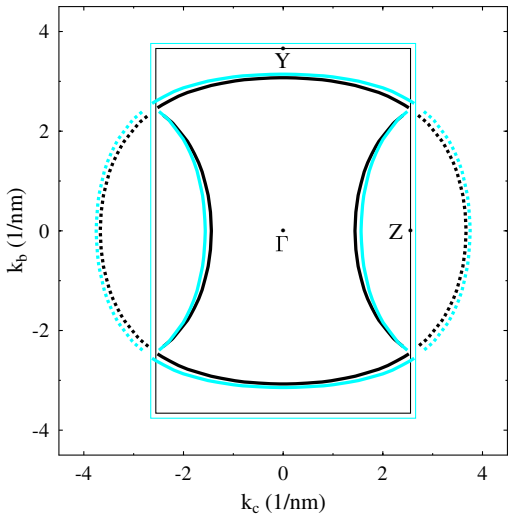

FIG. 3 (color online). Fermi surface cuts for nonmagnetic κ-(BEDT-TTF)$_2$Cu$_2$(CN)$_3$ at ambient pressure (black) and at $P = 0.75$ GPa (light). Thin lines show the respective first Brillouin zone. The combined elliptical orbit as detected by AMRO measurements (see text) is indicated by broken lines.

In the next step, we use the density functional theory (DFT) band structures to extract the parameters of the Hubbard Hamiltonian

$$H = \sum_{\langle ij\rangle,\sigma} t(c^{\dagger}_{i\sigma}c_{j\sigma} + \text{H.c.}) + \sum_{[ij],\sigma} t'(c^{\dagger}_{i\sigma}c_{j\sigma} + \text{H.c.}) + U\sum_i \left(n_{i\uparrow} - \frac{1}{2}\right)\left(n_{i\downarrow} - \frac{1}{2}\right). \quad (1)$$

where $\langle ij\rangle$ and $[ij]$ indicate sums over nearest and next nearest neighbors, respectively. We do this by fitting the bands to a tight-binding model. Note that also nonlocal correlations V, V' are thought to play a role in organic CT salts but their determination is beyond the scope of our present investigation. We consider each molecule position as shown in Fig. 1(c) as a site; then the four (eight) sites per unit cell contribute the four (eight) ET bands at the Fermi level in the case of κ-CN and κ-SCN (κ-Br and κ-Cl). This yields the hopping integrals t_1 to t_4 where the index indicates increasing distance; t_1 is the intradimer hopping integral. The black lines in Fig. 2 show as an example the tight-binding fit obtained from the molecular model. We follow Ref. [13] in the use of the geometrical formulas $t = (t_2 + t_4)/2$ and $t' = t_3/2$ for obtaining t and t' of Eq. (1). In order to corroborate these results, we use the alternative method of considering the ET dimers as sites of the tight-binding model as shown in Fig. 1(d). Then the two dimers per unit cell for κ-CN and κ-SCN are responsible for the two antibonding ET bands at the Fermi level (or four dimers/four antibonding bands in the case of κ-Br and κ-Cl).

The result of these extensive band structure calculations and tight-binding fits is summarized in Fig. 4. The choice of basis set (LAPW or FPLO), functional (GGA or LDA), and number of sites included in the fit (molecules or dimers) results in a certain spread of resulting t, t' pairs which we interpret as a margin of error. The slopes of the lines connecting the origin with the tight-binding results for the GGA bands [31] show the results for the t'/t ratios at ambient pressure: $t'/t = 0.83 \pm 0.08$ for κ-CN, $t'/t = 0.58 \pm 0.05$ for κ-SCN, $t'/t = 0.44 \pm 0.05$ for κ-Cl, and $t'/t = 0.42 \pm 0.08$ for κ-Br.

With the tight-binding results, we can estimate the Hubbard U as $U \approx 2t_1$ following Ref. [32]. We obtain U/t ratios of $U/t = 7.3$ for κ-CN, $U/t = 6.0$ for κ-SCN, $U/t = 5.5$ for κ-Cl and $U/t = 5.1$ for κ-Br. These values provide a readjustment of the position of the four κ-type CT salts in the $(U/t, t'/t)$ phase diagram, compared to the semiempirical calculations: For κ-CN, we replace (8.2, 1.06) by (7.3, 0.83), for κ-SCN (6.8, 0.84) by (6.0, 0.58), for κ-Cl (7.5, 0.75) by (5.5, 0.44) and for κ-Br (7.2, 0.68) by (5.1, 0.42). At $P = 0.75$ GPa, we have (6.0, 0.75) for κ-CN and (5.7, 0.58) for κ-SCN.

In Fig. 4 we also show the analysis of pressure effects on the t, t' parameters. We represented with arrows the parameter changes from the ambient pressure results to the $P = 0.75$ GPa results in κ-SCN and κ-CN. For κ-CN, pressure leads to a decrease in the t'/t ratio, while we observe almost constant t'/t for κ-SCN. On the other hand we can establish that the parameter differences among the three studied cases at ambient pressure can be

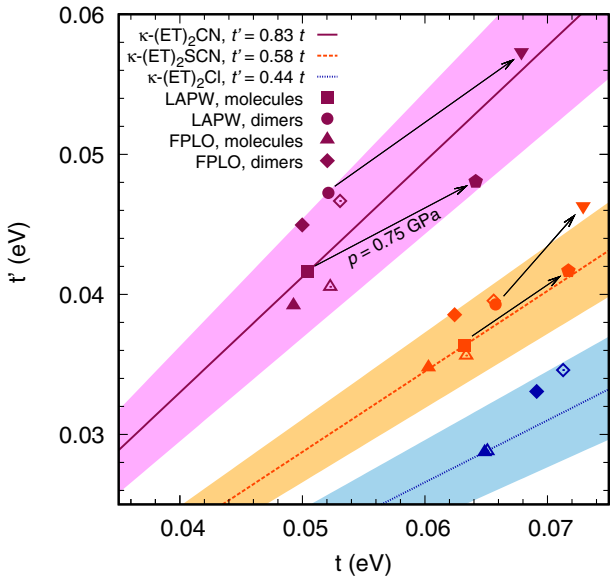

FIG. 4 (color online). Overview of hopping parameters obtained from GGA (filled symbols) and LDA (open symbols) calculations for κ-(BEDT-TTF)$_2$Cu$_2$(CN)$_3$, κ-(BEDT-TTF)$_2$Cu(SCN)$_2$, and κ-(BEDT-TTF)$_2$Cu[N(CN)$_2$]Cl. The spread of t and t' parameters depending on basis set, functional, and number of fitted bands yields t'/t ratios with a margin of error indicated by lines and shaded regions. Arrows indicate the change of t'/t ratio due to application of a pressure of $P = 0.75$ GPa.

attributed to internal chemical pressure due to the different anion sizes. By comparing the ratios t'/t for κ-CN, κ-SCN and κ-Cl at ambient pressure with the physical pressure t'/t behavior for κ-CN and κ-SCN we observe that chemical pressure and physical pressure have the same effect on the t'/t ratio: for κ-CN, pressure significantly decreases the t'/t ratio. This effect is weaker for κ-SCN.

We now consider the new positioning of the four κ-type CT salts in some of the calculated (U/t, t'/t) phase diagrams. In the PIRG phase diagram of Ref. [6], κ-Cl are shifted from the nonmagnetic insulating (NMI) phase to the antiferromagnetic insulating (AFI) phase which is an improvement as the superconducting phase is not considered in this work. Meanwhile, κ-CN and κ-SCN are only repositioned within the NMI phase. In the CDMFT phase diagram of Ref. [9], κ-Br is moved from the AF phase to the d-wave superconducting (SC) phase; κ-Cl is moved from the spin liquid (SL) phase to the border between AF and d-wave superconducting (SC) phase. κ-CN is moved from the d-wave SC phase to the border between SL and SC phases, and κ-SCN is moved within the SC phase. The effect of pressure means that κ-CN is moved diagonally across the SC phase by the application of $P = 0.75$ GPa. In particular, the positions of κ-Br, κ-Cl, and κ-CN in the phase diagram are clearly improved. Our results exclude the possibility of viewing κ-CN as a quasi-one-dimensional system [33].

In conclusion, we have presented the results of density functional theory calculations for four κ-type charge transfer salts. We obtain important shifts of the familiar t'/t ratios from semiempirical electronic structure calculations [13] towards significantly smaller values, i.e., towards lower frustration. Because of the smaller overall band width of the ET bands at the Fermi level, our estimate for the U/t values is also below the prevalent values. Our results call for a reexamination of the description of the κ-type charge transfer salts, and, in particular, for κ-CN, namely, which is the nature of the spin liquid at ambient pressure as well as the phase transition from Mott insulator to superconducting state under pressure.

We acknowledge useful discussions with E. Koch, L. Tocchio, and C. Gros. We thank the Deutsche Forschungsgemeinschaft for financial support through the TRR/SFB 49 and Emmy Noether programs and we acknowledge support by the Frankfurt Center for Scientific Computing.

Note added.—While finalizing this manuscript, Nakamura *et al.* [34] have posted a manuscript, where similar values of t'/t for κ-CN and κ-SCN as in our full-potential calculations are obtained from a pseudopotential method.

*jeschke@itp.uni-frankfurt.de

[1] BEDT-TTF, or shorter ET, stands for bis(ethylene-dithio) tetrathiafulvalene.

[2] H. Elsinger *et al.*, Phys. Rev. Lett. **84**, 6098 (2000).
[3] Y. Shimizu *et al.*, Phys. Rev. Lett. **91**, 107001 (2003).
[4] Y. Kurosaki *et al.*, Phys. Rev. Lett. **95**, 177001 (2005).
[5] F. Kagawa *et al.*, Nature (London) **436**, 534 (2005).
[6] H. Morita *et al.*, J. Phys. Soc. Jpn. **71**, 2109 (2002).
[7] R. T. Clay *et al.*, Phys. Rev. Lett. **101**, 166403 (2008).
[8] T. Watanabe *et al.*, J. Phys. Soc. Jpn. **75**, 074707 (2006); Phys. Rev. B **77**, 214505 (2008).
[9] B. Kyung and A.-M. S. Tremblay, Phys. Rev. Lett. **97**, 046402 (2006).
[10] T. Ohashi *et al.*, Phys. Rev. Lett. **100**, 076402 (2008).
[11] H. Lee *et al.*, Phys. Rev. B **78**, 205117 (2008).
[12] B. J. Powell and R. H. McKenzie, J. Phys. Condens. Matter **18**, R827 (2006).
[13] T. Komatsu *et al.*, J. Phys. Soc. Jpn. **65**, 1340 (1996).
[14] A. Fortunelli and A. Painelli, J. Chem. Phys. **106**, 8051 (1997); Phys. Rev. B **55**, 16088 (1997).
[15] R. Car and M. Parrinello, Phys. Rev. Lett. **55**, 2471 (1985).
[16] P. E. Blöchl, Phys. Rev. B **50**, 17953 (1994).
[17] M. Parrinello and A. Rahman, Phys. Rev. Lett. **45**, 1196 (1980).
[18] P. Blaha *et al.* *WIEN2K, An Augmented Plane Wave + Local Orbitals Program for Calculating Crystal Properties* (Karlheinz Schwarz/Techn. Universität Wien, Wien, Austria, 2001).
[19] K. Koepernik and H. Eschrig, Phys. Rev. B **59**, 1743 (1999); http://www.FPLO.de.
[20] U. Geiser *et al.*, Inorg. Chem. **30**, 2586 (1991).
[21] For CP-PAW, we employ a $(4 \times 4 \times 4)$ k mesh and plane wave cutoffs of 60 and 240 Ry for the wave function and charge density, respectively.
[22] In the constant pressure [17] CPMD method, the pressure P directly enters the Lagrangian for the lattice dynamics as a term $P\Omega$ with unit cell volume Ω.
[23] M. Rahal *et al.*, Acta Crystallogr. Sect. B **53**, 159 (1997).
[24] U. Geiser *et al.*, Acta Crystallogr. Sect. C **47**, 190 (1991).
[25] A. M. Kini *et al.*, Inorg. Chem. **29**, 2555 (1990).
[26] J. M. Williams *et al.*, Inorg. Chem. **29**, 3272 (1990).
[27] For LAPW, we employ a $(5 \times 10 \times 7)$ k mesh in the irreducible wedge of the Brillouin zone, integrated by tetrahedron method [28] and a value $R_{\mathrm{MT}} \times k_{\mathrm{max}} = 3.37$ due to the presence of hydrogen.
[28] P. E. Blöchl *et al.*, Phys. Rev. B **49**, 16223 (1994).
[29] FPLO convergency was tested with up to 350 k points in the full Brillouin zone, using the tetrahedron method [28].
[30] E. Ohmichi *et al.*, J. Phys. Soc. Jpn. **66**, 310 (1997).
[31] The lines are connecting the origin with the results corresponding to the tight-binding fit to four LAPW GGA (eight FPLO GGA) bands for κ-CN and κ-SCN (κ-Cl), and the shaded regions containing all other results represent the possible deviation.
[32] R. H. McKenzie, Comments Condens. Matter Phys. **18**, 309 (1998).
[33] Y. Hayashi and M. Ogata, J. Phys. Soc. Jpn. **76**, 053705 (2007).
[34] K. Nakamura *et al.*, arXiv:0903.5409.